# Time-Resolved Electron Diffraction from Selectively Aligned Molecules

Peter Reckenthaeler,[1,2] Martin Centurion,[1] Werner Fuß,[1] Sergei A. Trushin,[1] Ferenc Krausz,[1,2] and Ernst E. Fill[1]

[1]*Max-Planck-Institut für Quantenoptik, Hans-Kopfermann-Straße 1, D-85748 Garching, Germany*

[2]*Ludwig-Maximilians-Universität München, Am Coulombwall 1, D-85748 Garching, Germany*

(Received 27 March 2009; published 27 May 2009)

We experimentally demonstrate ultrafast electron diffraction from transiently aligned molecules in the absence of external (aligning) fields. A sample of aligned molecules is generated through photodissociation with femtosecond laser pulses, and the diffraction pattern is captured by probing the sample with picosecond electron pulses shortly after dissociation—before molecular rotation causes the alignment to vanish. In our experiments the alignment decays with a time constant of $2.6 \pm 1.2$ ps.

DOI: 10.1103/PhysRevLett.102.213001 PACS numbers: 33.15.Mt, 07.78.+s, 33.15.Bh, 82.53.Eb

*Introduction.*—Determination of structure and dynamics using isolated molecules is important for obtaining accurate information, with the molecules free of external forces and intermolecular interactions. Electron diffraction has been very successful in determining the structure of molecules in the gas phase, owing to the large scattering cross section between electrons and atoms [1]. However, due to the random orientation of the molecules in the gas phase only 1D information (the interatomic distances) can be extracted from the diffraction patterns, which limits the size of molecular structures that can be studied.

The technique of x-ray crystallography has been successful in studying larger molecules. For example, the majority of the known protein structures have been determined by x-ray diffraction from crystallized samples [2]. This technique, however, is limited to the fraction of molecules that can be crystallized. Additionally, crystallized molecules are subject to strong fields that constrain their conformation and hamper the study of dynamics. Recently, a strategy was proposed in which a single molecule is exposed to a large enough number of photons within an x-ray laser pulse short enough to capture a diffraction pattern before the molecule is destroyed [3]. Diffraction images of $\mu$m and nm-sized objects have been recorded with femtosecond soft-x-ray pulses [4,5]. However, this approach currently relies on large-scale facilities.

An alternative approach consists in recording a diffraction pattern from an ensemble of aligned molecules in the gas phase. It has been shown theoretically that electron diffraction from aligned molecules in the gas phase reveals not only the interatomic distances but also the corresponding angles [6,7]. Aligning molecules in helium droplets using powerful cw lasers has been proposed [8], and electron diffraction from adiabatically aligned molecules has been demonstrated experimentally [9]. However, the presence of strong alignment fields can affect the structure and dynamics of the molecules under investigation and prevents the study of field-free molecules. To overcome this problem, we propose using a sample of nonadiabatically aligned molecules in which the alignment field is no longer present at the time the diffraction pattern is recorded. Molecules can be aligned by means of femtosecond laser pulses either via active laser alignment techniques [10] or selectively through a dissociation reaction [6]. This technique requires using ultrashort electron pulses to record the diffraction pattern before the alignment vanishes. Ultrafast electron diffraction experiments have been performed with picosecond resolution for gas phase experiments [11] and femtosecond resolution in solid-state experiments [12,13], but so far the possibility of recording a diffraction pattern from field-free aligned molecules has not been demonstrated experimentally.

Here we show for the first time electron diffraction patterns recorded from a sample of transiently aligned molecules. In our experiments molecules are aligned selectively using photodissociation of $C_2F_4I_2$ (1,2-diiodotetrafluoroethane). The breaking of a molecular bond gives a clear signal in the time-resolved diffraction patterns, which simplifies the investigation of the transient alignment effect. The molecules are dissociated using a linearly polarized femtosecond laser pulse. The corresponding absorption cross section is proportional to $\cos^2(\alpha)$, where $\alpha$ is the angle between the laser polarization and the direction of the transition dipole moment (Fig. 1). For $C_2F_4I_2$ the transition dipole moment of the most intense transition is parallel to the C-I bond, along which the dissociation takes place. Therefore, the $C_2F_4I$ radicals emerge preferentially with the dissociated C-I direction aligned along the laser polarization vector. Note that by using circular polarization an aligned ensemble of undissociated molecules could be produced. Because of the rotations of the molecules the alignment decays with time. The time constants of the reaction have been determined using mass spectrometry [14]:

$$C_2F_4I_2 \xrightarrow{200\ \mathrm{fs}} C_2F_4I + I \xrightarrow{25\ \mathrm{ps}} C_2F_4 + 2I.$$

The first iodine atom breaks off within 200 fs, leading to the intermediate $C_2F_4I$ radical, which subsequently fragments within some 25 ps to yield $C_2F_4$. The structure of the intermediate $C_2F_4I$ has been determined using ultrafast electron diffraction (UED) [11].

 

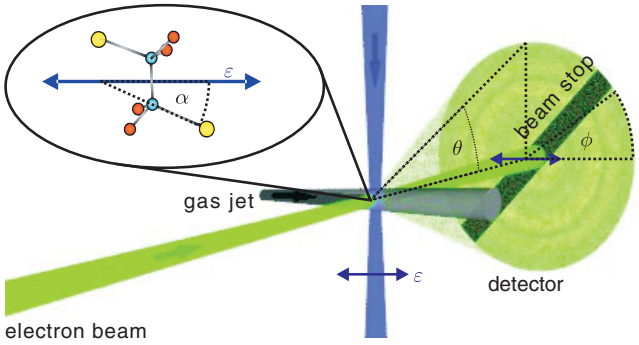


FIG. 1 (color). Experimental geometry: the electron beam, laser beam, and gas jet are mutually orthogonal. The polarization of the laser beam is orthogonal to the direction of propagation of the electron beam. $\theta$ is the scattering angle and $\phi$ is the azimuthal detector angle with respect to the laser polarization. $\vec{\varepsilon}$: laser polarization (blue arrow), $C_2F_4I_2$ molecule (schematic); $\alpha$: angle between the C-I bond (dissociation axis) and laser polarization. The constituent atoms are color coded, with yellow for iodine, light blue for carbon, and red for fluorine.

*Experimental setup.*—The experimental geometry is shown in Fig. 1 (for more detail, see [15]). A supersonic gas jet is introduced into a vacuum chamber using a Laval nozzle. It consists of $C_2F_4I_2$ molecules seeded in helium for rotational cooling. The rotational temperature is calculated to be 168 K for our gas jet using an empirical formula [16]. 50 fs laser pulses at a central wavelength of 800 nm and a repetition rate of 1 kHz are frequency tripled to produce UV pulses with an energy of 100 $\mu$J at a central wavelength of 267 nm. These UV pulses are focused to a 200-$\mu$m diameter inside the gas jet to initiate the dissociation reaction. A small fraction of the fundamental laser pulse energy is split off and used to trigger electron emission from a photocathode. The ejected electron pulse (containing some 10 000 electrons) is accelerated to 29 keV before traversing the gas jet. The electron beam, laser beam, and gas jet are mutually orthogonal. The directly transmitted electron beam is blocked and the diffraction pattern is recorded using a phosphor screen fiber-coupled to a CCD camera. The duration of the electron pulse on target was calculated to be 2.3 ps using the general particle tracer code [17]. Because of the velocity mismatch between the electron and the laser pulses the total time resolution of our system is 4 ps [15].

*Theory.*—In the analysis of gas electron diffraction patterns [18], the diffracted electron intensity ($I_{\mathrm{tot}}$) is written as the sum of two contributions, the ensemble-averaged atomic ($I_{\mathrm{at}}$) and molecular ($I_{\mathrm{mol}}$) scattering intensities: $I_{\mathrm{tot}}(s) = I_{\mathrm{at}}(s) + I_{\mathrm{mol}}(s)$. $I_{\mathrm{at}}$ accounts for elastic scattering from the constituent atoms, while $I_{\mathrm{mol}}$ arises from the interference of waves scattered from pairs of atoms. Here $s = 4\pi \sin(\theta/2)/\lambda$ is the magnitude of the momentum transfer between incident and diffracted electrons, $\theta$ and $\lambda$ denote the scattering angle and the electron wavelength; in our experiment $\lambda = 0.07$ Å.

In the general case of anisotropic samples, the diffraction patterns are not cylindrically symmetric but depend on the azimuthal detector angle $\phi$. The ensemble-averaged molecular scattering intensity can be written as

$$I_{\mathrm{mol}}(s, \phi) \propto \sum_{i=1}^{N} \sum_{\substack{j=1 \\ i \neq j}}^{N} |f_i||f_j| \cos(\eta_i - \eta_j) F_{ij}(s, \phi). \quad (1)$$

Here, $|f_i|$ is the elastic scattering amplitude for atom $i$, $\eta_i$ represents the phase shift suffered by the respective scattered wave. The factor $F_{ij}$ incorporates the effects of alignment. In the case of selective alignment through photodissociation it reads [7]

$$F_{ij}(s, \phi) = \frac{j_1(sr_{ij})}{sr_{ij}} - \left[\sin^2(\Omega_{ij}) + (2\text{–}3\sin^2(\Omega_{ij}))\cos^2\left(\frac{\theta}{2}\right)\cos^2(\phi)\right]\frac{j_2(sr_{ij})}{sr_{ij}}, \quad (2)$$

where $r_{ij}$ is the internuclear distance between atoms $i$ and $j$, $j_l$ is the spherical Bessel function of order $l$, and $\Omega_{ij}$ is the angle between $r_{ij}$ and the laser polarization. For isotropic samples $F_{ij}(s, \phi)$ is replaced by $\sin(sr_{ij})/(sr_{ij})$, and the $\phi$ dependence vanishes. It is common usage to depict the diffraction patterns in the form of modified scattering intensities $sM(s, \phi) = s \cdot I_{\mathrm{mol}}(s, \phi)/I_{\mathrm{at}}(s)$ to compensate for the rapid drop of the scattering signal with increasing $s$. Azimuthal averaging of $sM(s, \phi)$ patterns from isotropic samples results in the one-dimensional $sM(s)$ function. The sine Fourier transform of $sM(s)$ yields the radial distribution function $f(r)$, which peaks at the interatomic distances [18].

*Static diffraction patterns.*—The experimental and theoretical $sM(s)$ and the corresponding $f(r)$ functions for $C_2F_4I_2$ are shown in Figs. 2(a) and 2(b), respectively (for details on the data analysis, see Ref. [15]). The calculated curve draws on structural parameters from the literature

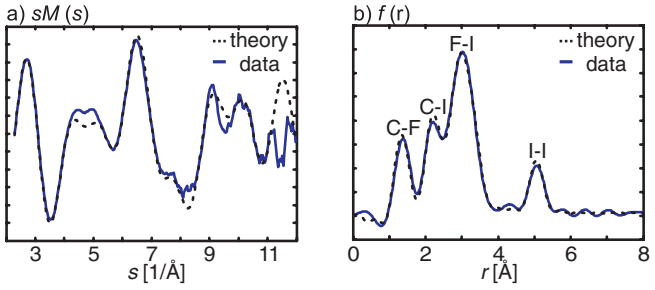


FIG. 2 (color online). Ground-state results for $C_2F_4I_2$. (a) Azimuthally averaged $sM$ functions, from experiment (blue or gray line) and theory (dotted black line). (b) Corresponding radial distribution functions $f(r)$. The dominant contributions to the peaks are labeled.

[19–21]. The experimental $sM(s)$ agrees well with the theoretical prediction and results published previously [11,19] up to $s \approx 10$ Å$^{-1}$, where the signal drops below the noise level. In Fig. 2(b) the distances which contribute dominantly to the peaks are indicated. Because of the finite $s$-range accessible some of the peaks corresponding to different internuclear distances overlap.

*Time-resolved diffraction experiments.*— Figures 3(a)–3(c) show the results of our pump-probe measurements in terms of the difference $\Delta[sM(s, \phi, t)]$ between $sM(s, \phi, t)$ patterns measured at a certain delay $t$ after the laser dissociation and the ground-state pattern shown in Fig. 2(a). We define the zero of time at the delay $t$ between electron and laser pulses for which the first changes become visible. Figure 3(a) shows $\Delta[sM(s, \phi, t)]$ close to $t = 0$. At this early time step the dissociation signal is small due to our instrument response time; however, the pattern shows significant anisotropy. The intensity of the image is higher along the direction of laser polarization, indicating that the dissociated molecules are aligned along the direction of laser polarization. The theoretical part of this figure [calculated with Eqs. (1) and (2) assuming that one-third of the molecules are dissociated to $C_2F_4I$] shows a similar pattern. Using the results shown in Fig. 3(a), we calculate the degree of alignment of the $C_2F_4I$ radical to be $\langle \cos^2(\alpha) \rangle = 0.5$. This quantity represents the average molecular alignment with respect to the laser polarization. Values of $\langle \cos^2(\alpha) \rangle = 1/3$ and $\langle \cos^2(\alpha) \rangle = 1$ represent an isotropic distribution and perfect alignment, respectively, while a perfect cosine square distribution would result in a value of 0.6. Figure 3(b) shows results at a later time when the anisotropy is weaker but still clearly visible. The corresponding theoretical pattern was calculated using a weighted average between the anisotropic pattern and the isotropic theory, assuming that 2/3 of the molecular orientations have randomized. Figure 3(c) shows $\Delta[sM(s, \phi, t)]$ for later time steps. The pattern becomes isotropic; i.e., the alignment is lost due to the molecular rotations. The theoretical pattern shown in Fig. 3(c) was generated using the isotropic theory assuming that all the $C_2F_4I$ radicals have decayed to $C_2F_4$.

We now turn to a quantitative analysis of the diffraction patterns. Because of the anisotropy we restrict the averaging to narrow pairs of cones aligned parallel and perpendicularly to the laser polarization, yielding $\Delta[sM_{||}(s, t)]$ and $\Delta[sM_{\perp}(s, t)]$, respectively. The results are shown in Fig. 4(a). To display the noise level of the data the figure contains time steps before the dissociation ($t < 0$) which show no significant difference in the signal diffracted parallel and perpendicular to the laser polarization. The plots recorded within less than 2 ps following excitation clearly reveal a significant difference, indicating the anisotropy. The difference vanishes completely at $t > 8$ ps.

We now use $\Delta[sM_{||}(s, t)]$ and $\Delta[sM_{\perp}(s, t)]$ to determine the temporal evolution of the anisotropy. As an approximation we define corresponding scattering signal amplitudes $A_{||}(t)$ and $A_{\perp}(t)$ within a limited $s$ range ($2.2 < s < 6.2$) where the $s$ dependencies of $\Delta[sM_{||}(s, t)]$ and $\Delta[sM_{\perp}(s, t)]$ are similar. The time dependencies of $A_{||}(t)$ and $A_{\perp}(t)$ are shown in Fig. 4(b).

While the rise time is similar for $A_{||}(t)$ and $A_{\perp}(t)$, there is a clear delay between the two curves, with the signal along the laser polarization [$A_{||}(t)$] appearing first. This is due to the fact that the $C_2F_4I$ radicals remain aligned immediately after the dissociation. Shortly thereafter, the alignment deteriorates due to the molecular rotation. Note that the delay between the two signals can be measured with a resolution well beyond the instrumental response time of 4 ps without deconvolution. After 8 ps, the orientations have fully randomized and the difference between $A_{||}(t)$ and $A_{\perp}(t)$ vanishes.

Finally, we quantify the anisotropy using the following definition [Fig. 4(c)]:

$$\delta(t) = \frac{A_{||}(t) - A_{\perp}(t)}{A_{||}(t) + A_{\perp}(t)}. \tag{3}$$

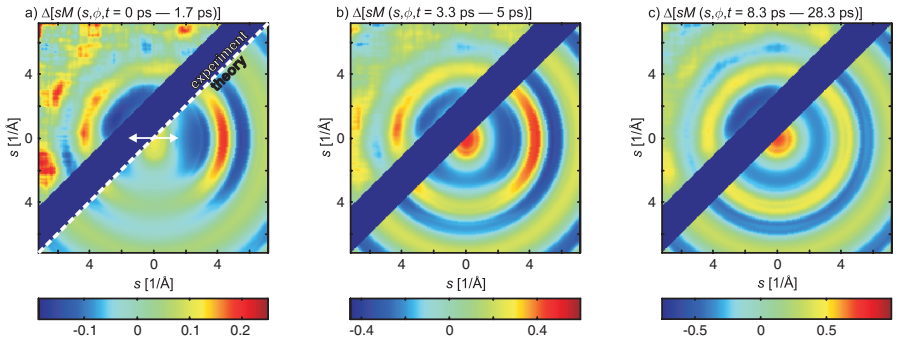


FIG. 3 (color). 2D time-resolved diffraction patterns. (a) $\Delta[sM(s, \phi)]$ close to zero delay of probe: the pattern is the result of averaging patterns recorded within the delay range of $t = 0$ ps and $t = 1.7$ ps. The white arrow indicates the direction of the laser polarization. The upper left half of the image displays the experimental data, while the lower right half shows the theoretical prediction. The dark region splitting the image is the shadow of our beam stop. (b) $\Delta[sM](s, \phi)$ averaged between $t = 3.3$ ps and $t = 5$ ps. (c) $\Delta[sM](s, \phi)$ averaged between $t = 8.3$ ps and $t = 28.3$ ps.

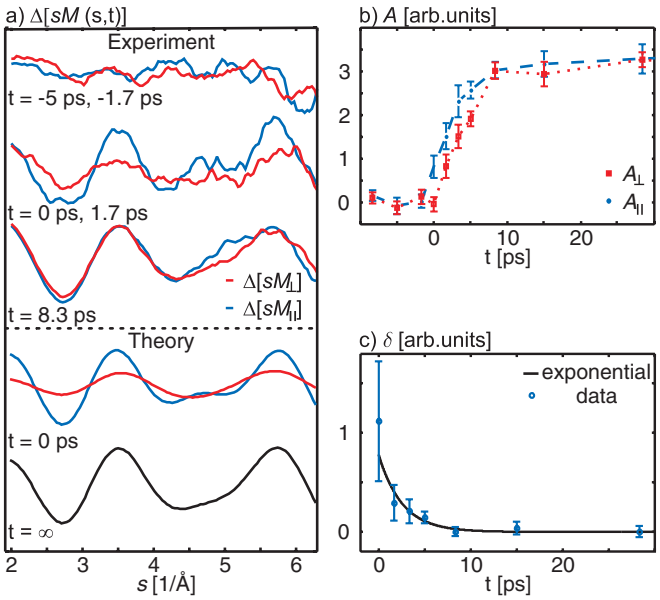


FIG. 4 (color). (a) Experiment: $\Delta[sM_{||}(s)]$ and $\Delta[sM_{\perp}(s)]$ before time zero (averaged between $t = -5$ ps and $t = -1.7$ ps), $\Delta[sM_{||}(s)]$ and $\Delta[sM_{\perp}(s)]$ close to time zero (averaged between $t = 0$ ps and $t = 1.7$ ps) and for late time steps (averaged between $t = 8.3$ ps and $t = 28.3$ ps). For visual clarity the curves for $t = -5$ ps, $-1.7$ ps, and for $t = 0$ ps, 1.7 ps are multiplied by a factor of 2.8. Theory: corresponding theory curves. (b) $A_{||}$ and $A_{\perp}$ measured parallel and perpendicular to the laser polarization as functions of delay time $t$; (c) Anisotropy parameter $\delta$ as a function of delay time $t$; the black line shows an exponential fit to the data.

From an exponential fit to the data we measured a dephasing time of the alignment of $2.6 \pm 1.2$ ps. This is in good agreement with the theoretical value of 2.7 ps, calculated as in Ref. [22].

*Conclusion.*—Our results demonstrate for the first time the feasibility of recording a UED pattern from transiently aligned molecules. The decay of the alignment was measured on a picosecond time scale. These results are a first important step towards 3D imaging of complicated molecular structures with electron diffraction or possibly using the new generation hard x-ray sources. Increasing the degree of alignment, combined with diffraction patterns corresponding to different projections of the molecule (using suitable algorithms [23]), will allow full 3D measurement of the molecular structure. This method could also be applied to investigate ultrafast molecular dynamics in a field-free environment. Improving transient molecular alignment may be pursued by saturating the dissociation [24] or with active 1D [25] and even 3D alignment techniques [26,27]. The temporal resolution could be further improved by compressing the electron pulses to a few femtoseconds [28,29].

This work was supported by DFG under Contract No. SFB Transregio 6039 and by the DFG Cluster of Excellence "Munich Centre for Advanced Photonics." P. R. is supported by the International Max Planck Research School on Advanced Photon Science—IMPRS-APS [30]. M. C. was supported by the Alexander von Humboldt Foundation. S. A. T. thanks the Deutsche Forschungsgemeinschaft for financial support (project FU 363/1).

[1] R. Henderson, Q. Rev. Biophys. **28**, 171 (1995).
[2] H. M. Berman *et al.*, Acta Crystallogr. Sect. D **58**, 899 (2002).
[3] R. Neutze *et al.*, Nature (London) **406**, 752 (2000).
[4] H. N. Chapman *et al.*, Nature Phys. **2**, 839 (2006).
[5] M. J. Bogan *et al.*, Nano Lett. **8**, 310 (2008).
[6] J. C. Williamson and A. H. Zewail, J. Phys. Chem. **98**, 2766 (1994).
[7] J. S. Baskin and A. H. Zewail, Chem. Phys. Chem. **6**, 2261 (2005).
[8] J. C. H. Spence and R. B. Doak, Phys. Rev. Lett. **92**, 198102 (2004).
[9] K. Hoshina *et al.*, J. Chem. Phys. **118**, 6211 (2003).
[10] H. Stapelfeldt and T. Seideman, Rev. Mod. Phys. **75**, 543 (2003).
[11] H. Ihee *et al.*, Science **291**, 458 (2001).
[12] B. Siwick, J. Dwyer, R. Jordan, and R. J. Dwayne Miller, Science **302**, 1382 (2003).
[13] S. H. Nie, X. Wang, H. Park, R. Clinite, and J. Cao, Phys. Rev. Lett. **96**, 025901 (2006).
[14] D. Zhong, S. Ahmad, and A. H. Zewail, J. Am. Chem. Soc. **119**, 5978 (1997).
[15] See EPAPS Document No. E-PRLTAO-102-051923 for more details on the experimental setup, the data acquisition and processing, and on the experimental time response. For more information on EPAPS, see http://www.aip.org/pubservs/epaps.html.
[16] D. P. Pullman, B. Friedrich, and D. R. Herschbach, J. Chem. Phys. **93**, 3224 (1990).
[17] www.pulsar.nl
[18] L. Schäfer, Appl. Spectrosc. **30**, 123 (1976).
[19] H. Thomassen, S. Samdal, and K. Hedberg, J. Am. Chem. Soc. **114**, 2810 (1992).
[20] J. L. Carlos, R. R. Karl, and S. H. Bauer, J. Chem. Soc., Faraday Trans. **70**, 177 (1974).
[21] H. Ihee *et al.*, J. Phys. Chem. A **106**, 4087 (2002).
[22] W. Fuß *et al.*, J. Chem. Phys. **106**, 2205 (1997).
[23] J. R. Fienup, Appl. Opt. **21**, 2758 (1982).
[24] D. Magde, J. Chem. Phys. **68**, 3717 (1978).
[25] L. Holmegaard *et al.*, Phys. Rev. Lett. **102**, 023001 (2009).
[26] K. F. Lee, D. M. Villeneuve, P. B. Corkum, A. Stolow, and J. G. Underwood, Phys. Rev. Lett. **97**, 173001 (2006).
[27] J. J. Larsen, K. Hald, N. Bjerre, H. Stapelfeldt, and T. Seideman, Phys. Rev. Lett. **85**, 2470 (2000).
[28] E. Fill, L. Veisz, A. Apolonski, and F. Krausz, New J. Phys. **8**, 272 (2006).
[29] L. Veisz *et al.*, New J. Phys. **9**, 451 (2007).
[30] www.mpq.mpg.de/APS